2010-01-01

Role of muscle c-Jun NH2-terminal kinase 1 in obesity-induced insulin resistance

Guadalupe Sabio
University of Massachusetts Medical School

Et al.

MOLECULAR AND CELLULAR BIOLOGY, Jan. 2010, p. 106–115 Vol. 30, No. 1
0270-7306/10/$12.00 doi:10.1128/MCB.01162-09

Role of Muscle c-Jun NH_2-Terminal Kinase 1 in Obesity-Induced Insulin Resistance▽

Guadalupe Sabio,[1,2]† Norman J. Kennedy,[2] Julie Cavanagh-Kyros,[1,2] Dae Young Jung,[2] Hwi Jin Ko,[2] Helena Ong,[2] Tamera Barrett,[2] Jason K. Kim,[2,3] and Roger J. Davis[1,2]*

Howard Hughes Medical Institute,[1] Program in Molecular Medicine,[2] and Department of Medicine, Division of Endocrinology, Metabolism and Diabetes,[3] University of Massachusetts Medical School, Worcester, Massachusetts 01605

Received 28 August 2009/Returned for modification 5 October 2009/Accepted 13 October 2009

Obesity caused by feeding of a high-fat diet (HFD) is associated with an increased activation of c-Jun NH_2-terminal kinase 1 (JNK1). Activated JNK1 is implicated in the mechanism of obesity-induced insulin resistance and the development of metabolic syndrome and type 2 diabetes. Significantly, *Jnk1*$^{-/-}$ mice are protected against HFD-induced obesity and insulin resistance. Here we show that an ablation of the *Jnk1* gene in skeletal muscle does not influence HFD-induced obesity. However, muscle-specific JNK1-deficient (M^{KO}) mice exhibit improved insulin sensitivity compared with control wild-type (M^{WT}) mice. Thus, insulin-stimulated AKT activation is suppressed in muscle, liver, and adipose tissue of HFD-fed M^{WT} mice but is suppressed only in the liver and adipose tissue of M^{KO} mice. These data demonstrate that JNK1 in muscle contributes to peripheral insulin resistance in response to diet-induced obesity.

Obesity is a major risk factor for the development of insulin resistance, hyperglycemia, and metabolic syndrome that can lead to β-cell dysfunction and type 2 diabetes (8). The prevalence of human obesity represents a serious health problem in the United States. It is therefore important that we obtain a detailed understanding of the molecular mechanism that accounts for obesity-induced insulin resistance. Recent progress has led to the identification of signal transduction pathways that may mediate the effects of obesity on insulin resistance (14, 23).

c-Jun NH_2-terminal kinase 1 (JNK1) represents one signaling pathway that has been implicated in the pathogenesis of metabolic syndrome and type 2 diabetes (21). JNK1 is activated when mice are fed a high-fat diet (HFD) (7). Moreover, *Jnk1*$^{-/-}$ mice are protected against HFD-induced insulin resistance (7). The mechanism of protection is mediated, in part, by the failure of *Jnk1*$^{-/-}$ mice to develop HFD-induced obesity (7). However, JNK1 can regulate insulin resistance independently of obesity. Thus, mice with an adipose tissue-specific JNK1 deficiency develop normal diet-induced obesity but exhibit selective protection against HFD-induced insulin resistance in both the liver and adipose tissue (16). These data indicate that adipose tissue JNK1 plays a critical role during the development of HFD-induced insulin resistance.

The liver plays a key role in the insulin-stimulated disposal of blood glucose during the postprandial state because of reduced gluconeogenesis and increased glycogen synthesis (17). However, glucose uptake by skeletal muscle also makes a major contribution to insulin-stimulated glucose disposal (17). Muscle may therefore be an important target of obesity-induced JNK1 signaling and the regulation of glucose homeostasis.

The purpose of this study was to test the role of JNK1 in muscle. Our approach was to examine the effect of a muscle-specific ablation of the *Jnk1* gene in mice. We found that HFD-fed control wild-type (M^{WT}) mice and muscle-specific JNK1-deficient (M^{KO}) mice became similarly obese. However, M^{KO} mice were selectively protected against HFD-induced insulin resistance. This analysis demonstrates that muscle JNK1 contributes to the effects of obesity on insulin resistance.

MATERIALS AND METHODS

Mice. We previously described *Jnk1*$^{-/-}$ mice (6) and *Jnk1*$^{LoxP/LoxP}$ mice (4). *Mck-Cre* mice (3) were obtained from the Jackson Laboratories. The mice were backcrossed to the C57BL/6J strain (Jackson Laboratories) and were housed in facilities accredited by the American Association for Laboratory Animal Care. The mice were genotyped by PCR analysis of genomic DNA (4). The animal studies were approved by the Institutional Animal Care and Use Committee of the University of Massachusetts Medical School.

RNA analysis. The expression of mRNA was examined by quantitative PCR analysis using a 7500 Fast real-time PCR machine (Applied Biosystems). TaqMan assays were used to quantitate *Cd68* (Mm00839636_g1), *C/ebp*α (Mm00514283_s1), *C/ebp*β (Mm00843434_s1), *Cyp2e1* (Mm00491127_m1), fatty acid synthase (*Fas*) (Mm00662322_g1), *Icam1* (Mm00516023_m1), *Ifn*-γ (Mm00801778_m1), *Il6* (Mm00446190_m1), *Il13* (Mm99999190_m1), lysozyme (*Lysz*) (Mm00727183_m1), *Lpl* (Mm00434770_m1), microsomal triglyceride transfer protein (*Mttp*) (Mm00435015_m1), *Pgc1*α (Mm00447183_m1), and *Tnfa* (Mm00443258_m1) (Applied Biosystems). The amounts of *Il10* mRNA (CTGGACAACATACTGCTAACCG and GGGCATCACTTCTACCAGGTAA), *Il12* mRNA (CCATTTTCCTTCTTGTGGAGCA and AGACATGGAGTCATAGGCTCTG), *Ppar*γ mRNA (TGTGGGGATAAAGCATCAGGC and CCGGCAGTTAAGATCACACCTA), *Pgc1*β mRNA (TACATGCATACCTACTGCCTGCCT and TTGGGCCAGAAGTTCCCTTAGGAT), *Srebp1* mRNA (GATGTGCGAACTGGACACCAG and CATAGGGGGCGTCAAACAG), and *Tgf*β*1* mRNA (TGGTTTGCCATCGTTTTGCTG and ACAGGTGAGGTTCACTGTTTCT) were examined by quantitative reverse transcription (RT)-PCR using Sybr green detection. The relative mRNA expression was normalized by measurement of the amount of *Gapdh* mRNA (4352339E) or 18S RNA (430449011032) in each sample using TaqMan assays (Applied Biosystems).

* Corresponding author. Mailing address: Howard Hughes Medical Institute, Program in Molecular Medicine, University of Massachusetts Medical School, 373 Plantation Street, Worcester, MA 01605. Phone: (508) 856-6054. Fax: (508) 856-3210. E-mail: Roger.Davis@Umassmed.edu.

† Present address: Departamento de Inmunología y Oncología, Centro Nacional de Biotecnología, CSIC, Campus de Cantoblanco-UAM, 28049 Madrid, Spain.

▽ Published ahead of print on 19 October 2009.

Immunoblot analysis. Tissue extracts were prepared by using Triton lysis buffer (20 mM Tris [pH 7.4], 1% Triton X-100, 10% glycerol, 137 mM NaCl, 2 mM EDTA, 25 mM β-glycerophosphate, 1 mM sodium orthovanadate, 1 mM phenylmethylsulfonyl fluoride, and 10 μg/ml of aprotinin and leupeptin). Extracts (20 to 50 μg of protein) were examined by protein immunoblot analysis by probing with antibodies to AKT, phospho-Thr^{308} AKT, and phospho-Ser^{473} AKT (Cell Signaling); IRS1 (16); phospho-Ser^{307} IRS1 (Millipore); and insulin receptor β subunit, JNK1, and glyceraldehyde-3-phosphate dehydrogenase (GAPDH) (Santa Cruz). Immunocomplexes were detected by enhanced chemiluminescence (NEN). Quantitation of immunoblots was performed by using the Odyssey infrared imaging system (Li-Cor Biosciences).

Measurement of glucose, adipokine, cytokine, and insulin concentrations in blood. The blood glucose concentration was measured with an Ascensia Breeze 2 glucometer (Bayer). Concentrations of adipokines, cytokines, and insulin in plasma were measured by enzyme-linked immunosorbent assay using a Luminex 200 machine (Millipore).

Glucose tolerance tests and ITTs. The mice were fed a standard chow diet or a HFD (Iso Pro 3000 [Purina] and catalog number F3282 [Bioserve Inc.]) for 16 weeks. Glucose tolerance tests and insulin tolerance tests (ITTs) were performed according to methods described previously (12).

Blood lipid analysis. Triglyceride was measured by using a kit purchased from Sigma. Cholesterol was measured by using a Cardiocheck PA instrument (PTS, Inc.). The concentration of free fatty acids was measured by using a kit purchased from Roche. Fast-performance liquid chromatography analysis of serum lipoproteins was performed by the University of Cincinnati Mouse Metabolic Phenotyping Center (Lipid, Lipoprotein, and Glucose Metabolism Core; P. Tso, Director).

Measurement of hepatic triglyceride content. The hepatic triglyceride content was measured using livers from mice fasted overnight. Total lipids were extracted from liver samples (50 mg) by using an 8:1 mixture of chloroform and methanol (4 h). The extracts were mixed with 1 N sulfuric acid and centrifuged (10 min). The amount of triglyceride was measured by using a kit purchased from Sigma.

Protein kinase assays. JNK activity was measured by using an in vitro protein kinase assay with c-Jun and [γ-^{32}P]ATP as substrates (22).

Hyperinsulinemic-euglycemic clamp studies. The clamp studies were performed at the University of Massachusetts Mouse Phenotyping Center. Briefly, mice were fed a HFD diet (55% fat by calories; Harlan Teklad) or chow diet for 4 weeks, and whole body fat and lean mass were noninvasively measured by using proton magnetic resonance spectroscopy (Echo Medical Systems). Following an overnight fast, a 2-h assay using a hyperinsulinemic-euglycemic clamp was conducted with conscious mice with a primed and continuous infusion of human insulin (priming with 150 mU/kg of body weight followed by 2.5 mU/kg/min) (Humulin; Eli Lilly), and 20% glucose was infused at variable rates to maintain euglycemia (10). Whole-body glucose turnover was assessed with a continuous infusion of [3-^{3}H]glucose, and 2-deoxy-D-[1-^{14}C]glucose (Perkin-Elmer) was administered as a bolus (10 μCi) at 75 min after the start of clamp studies to measure insulin-stimulated glucose uptake in individual organs. At the end of use of the clamps, mice were anesthetized, and tissues were taken for biochemical analysis (10).

Analysis of tissue sections. Histology was performed using tissue fixed in 10% formalin for 24 h, dehydrated, and embedded in paraffin. Sections (7 μm) were cut and stained using hematoxylin and eosin (American Master Tech Scientific). Immunohistochemistry was performed by staining tissue sections with an antibody to F4/80 (Abcam), a biotinylated secondary antibody (Biogenex), streptavidin-conjugated horseradish peroxidase (Biogenex), and the substrate 3,3′-diaminobenzidene (Vector Laboratories), followed by brief counterstaining with Mayer's hematoxylin (Sigma).

Statistical analysis. Differences between groups were examined for statistical significance using the Student test or analysis of variance with Fisher's test.

RESULTS

To test the role of JNK1 in muscle, we created mice without (M^{WT}) and with (M^{KO}) a selective defect in the expression of JNK1 in muscle (Fig. 1A). Measurement of JNK activity demonstrated that a HFD caused JNK activation in muscle, liver, and adipose tissue of control (M^{WT}) mice, but JNK activation was detected only in liver and adipose tissue of M^{KO} mice (Fig. 1B). Together, these data indicate that mice with a muscle-specific JNK1 deficiency represent a model for the analysis of muscle JNK1 deficiency.

Muscle-specific JNK1 deficiency does not affect diet-induced obesity. It is established that HFD-fed *Jnk1*$^{-/-}$ mice exhibit a severe defect in the development of obesity (7). We therefore tested whether a muscle-specific JNK1 deficiency might alter HFD-induced obesity. Comparison of chow-fed and HFD-fed M^{WT} and M^{KO} mice demonstrated that a muscle-specific JNK1 deficiency caused no defect in HFD-induced weight gain (Fig. 1C). Indeed, measurement of lean mass and fat mass by proton magnetic resonance spectroscopy demonstrated no significant differences between HFD-fed M^{KO} and M^{WT} mice (data not shown). This analysis demonstrated that a muscle JNK1 deficiency is not a major factor that contributes to the profound effect of a whole-body JNK1 deficiency on the suppression of HFD-induced obesity.

Feeding of an HFD caused hyperglycemia and hyperinsulinemia in mice, but no significant differences between M^{KO} and M^{WT} mice were detected (Fig. 2D to F). Glucose tolerance tests were performed to compare the responses of M^{KO} and M^{WT} mice to a glucose challenge. We found that the HFD caused glucose intolerance in both M^{KO} and M^{WT} mice (Fig. 2B). The HFD-induced glucose intolerance was caused, in part, by decreased glucose-induced insulin release. No significant differences between M^{KO} and M^{WT} mice were found in studies of glucose-induced insulin release (Fig. 2C). These data indicate that M^{KO} and M^{WT} mice mounted similar responses to a glucose challenge.

JNK1 deficiency in muscle did not affect the blood concentration of the adipokines leptin and resistin (Fig. 2G and H). However, analysis of the concentration of cytokines in the blood did indicate differences between M^{KO} and M^{WT} mice. Thus, the blood concentrations of the inflammatory cytokines tumor necrosis alpha (TNF-α), gamma interferon (IFN-γ), and interleukin-12 (IL-12) were greater in M^{KO} mice than in M^{WT} mice (Fig. 2I, J, and L). In contrast, no significant difference in the concentrations of the anti-inflammatory cytokine IL-10 in the blood was detected between M^{KO} and M^{WT} mice (Fig. 2K).

JNK1 deficiency causes increased insulin signaling in muscle. The insulin receptor substrate IRS-1 can be negatively regulated by the JNK-mediated phosphorylation of IRS-1 on Ser^{307} (1). We therefore anticipated that a loss of JNK1 in muscle would attenuate the negative regulatory phosphorylation of IRS-1 on Ser^{307} and increase the insulin-stimulated tyrosine phosphorylation of IRS-1. To test this hypothesis, we examined the effect of insulin treatment of M^{WT} and M^{KO} mice on insulin receptor and IRS-1 phosphorylation in muscle. We found that the JNK1 deficiency did not affect insulin receptor tyrosine phosphorylation or the amount of expression of the insulin receptor or IRS-1. However, the loss of JNK1 in muscle reduced the inhibitory phosphorylation of IRS-1 on Ser^{307} and increased the insulin-stimulated tyrosine phosphorylation of IRS-1 (Fig. 1D). These data suggest that JNK1 plays an important role in the regulation of IRS-1 and, therefore, insulin signal transduction in muscle.

Mice with a muscle-specific JNK1 deficiency exhibit increased insulin sensitivity. We performed an ITT to examine whether M^{KO} mice exhibit increased insulin sensitivity in vivo compared with M^{WT} mice (Fig. 2A). No significant differences between M^{KO} and M^{WT} mice were detected when these mice were fed a chow diet. In contrast, the HFD markedly suppressed the ITT response in M^{WT} mice, but HFD-fed M^{KO} mice re-

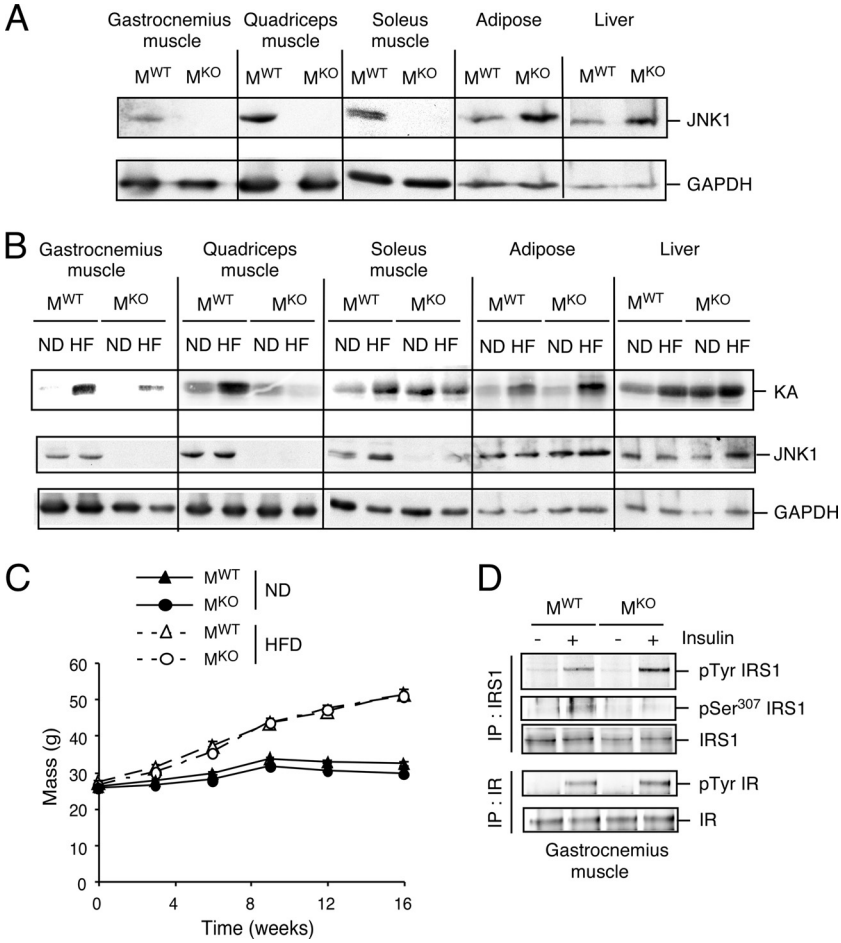

FIG. 1. Creation of mice with muscle-specific JNK1 deficiency. (A) Extracts prepared from epididymal fat (white adipose tissue), liver, and muscle (gastrocnemius, quadriceps, and soleus) of *Mck-Cre*$^{+}$ *Jnk1*$^{+/+}$ (M^{WT}) mice and *Mck-Cre*$^{+}$ *Jnk1*$^{LoxP/LoxP}$ (M^{KO}) mice were examined by immunoblot analysis by probing with antibodies to JNK1 and GAPDH. (B) M^{WT} and M^{KO} mice were fed a chow diet (ND) or HFD (HF) for 16 weeks and then fasted overnight. JNK protein activity in epididymal fat (adipose tissue), liver, and muscle was measured in a protein kinase (KA) assay using c-Jun and [γ-^{32}P]ATP as substrates. The cell extracts used for the protein kinase assay were also examined by immunoblot analysis by probing with antibodies to JNK1 and GAPDH. (C) Male M^{WT} and M^{KO} mice (8 to 10 weeks old) were fed either a chow diet (ND) or HFD for 16 weeks. The body weight of the mice was measured (means ± standard deviations [SD]) ($n = 10$). No significant difference between the body weights of M^{WT} and M^{KO} mice was detected ($P > 0.05$). (D) Chow-fed M^{WT} and M^{KO} mice were fasted overnight and then treated by intraperitoneal injection of 1.5 mU/kg insulin. Extracts prepared from gastrocnemius muscle at 10 min postinjection were examined by immunoblot analysis using antibodies to the insulin receptor (IR), IRS-1, phospho-Tyr, and IRS-1-Ser^{307}. IP, immunoprecipitation.

mained insulin sensitive (Fig. 2A). These data suggest that M^{KO} mice exhibit protection against HFD-induced insulin resistance.

To confirm the conclusion that M^{KO} mice are more insulin sensitive, we conducted a hyperinsulinemic-euglycemic clamp study with conscious mice following 4 weeks of feeding of a HFD or chow diet. The level of insulin-stimulated whole-body glucose turnover was modestly but significantly elevated in M^{KO} mice compared with M^{WT} mice following feeding of a chow diet or HFD (Fig. 3A). Whole-body glycolysis rates tended to be higher in chow-fed M^{KO} mice than in chow-fed M^{WT} mice ($P = 0.057$), but whole-body glycogen plus lipid synthesis rates were not altered in M^{KO} mice (Fig. 3B and C). No statistically significant differences in basal or clamp glucose concentrations (data not shown), hepatic glucose production (HGP) at the basal state or during the insulin-stimulated (clamp) state, and hepatic insulin action were detected between M^{KO} and M^{WT} mice (Fig. 3D to F). The level of insulin-stimulated muscle glucose uptake was significantly reduced in HFD-fed M^{WT} mice compared with chow-fed M^{WT} mice, but muscle glucose uptake in HFD-fed M^{KO} mice was similar to that of chow-fed M^{KO} mice (Fig. 3G). In contrast, the HFD caused a similar decrease in levels of insulin-stimulated glucose uptake by adipose tissue in M^{KO} and M^{WT} mice (Fig. 3H). These data demonstrate that M^{KO} mice exhibit a selective increase in skeletal muscle insulin sensitivity.

To obtain biochemical evidence for peripheral insulin sensitivity, we examined insulin-stimulated AKT activation in muscle, liver, and adipose tissue of M^{KO} and M^{WT} mice (Fig. 4). Insulin treatment of chow-fed M^{KO} and M^{WT} mice caused increased AKT activation. Feeding of an HFD suppressed insulin-stimulated AKT activation in the liver and adipose tissue of both M^{KO} and M^{WT} mice (Fig. 4B and C). In contrast, the HFD suppressed insulin-stimulated AKT

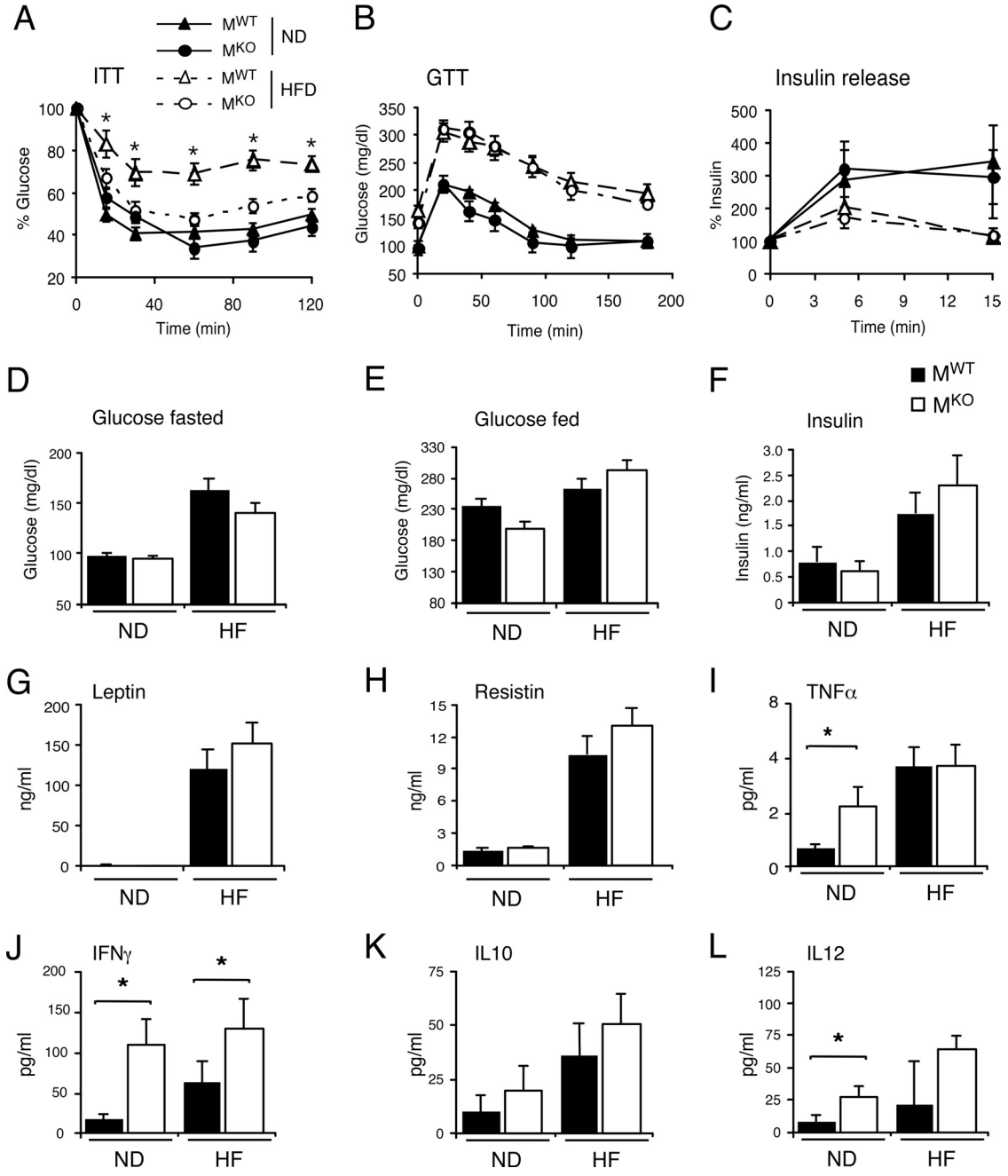

FIG. 2. Effect of muscle-specific JNK1 deficiency on diet-induced obesity. (A) ITTs of M^{WT} and M^{KO} male mice fed either a chow diet (ND) or an HFD for 16 weeks were performed by intraperitoneal injection of insulin (1.5 U/kg body mass). The concentration of blood glucose was measured (means ± SD) ($n = 10$). Statistically significant differences between M^{KO} and M^{WT} are indicated (*, $P < 0.05$). (B) Glucose tolerance tests (GTT) with chow-fed (ND) and HFD-fed M^{WT} and M^{KO} mice were performed by measurement of blood glucose concentrations in animals following intraperitoneal injection of glucose (1 g/kg). The data presented represent the means ± SD ($n = 10$ to ~15). No statistically significant differences between M^{WT} and M^{KO} mice were detected ($P > 0.05$). (C) Glucose-induced insulin release. The effect of the administration of glucose (2 g/kg body mass) by intraperitoneal injection on blood insulin concentrations was examined (means ± SD) ($n = 13$ to ~15). No statistically significant differences between M^{WT} and M^{KO} mice were detected ($P > 0.05$). (D and E) Chow-fed and HFD-fed (HF) M^{WT} and M^{KO} mice were fasted overnight (D) or fed ad libitum (E), and the blood glucose concentration was measured (mean ± SD) ($n = 10$ to ~15). No statistically significant differences were detected ($P > 0.05$). (F to L). The concentrations of insulin, adipokines, and cytokines in blood of chow-fed (ND) and HFD-fed (HF) M^{WT} and M^{KO} mice fasted overnight were measured by enzyme-linked immunosorbent assay (means ± SD) ($n = 10$ to ~15). Statistically significant differences are indicated (*, $P < 0.05$).

activation in muscle of M^{WT} mice but not M^{KO} mice (Fig. 4A). These data support the conclusion that M^{KO} mice exhibit a selective rescue from HFD-induced skeletal muscle insulin resistance.

Systemic effects of muscle-specific JNK1 deficiency. The ablation of the *Jnk1* gene in muscle may lead to changes in other tissues. Indeed, a comparison of the livers of M^{WT} and M^{KO} mice demonstrated that a muscle JNK1 deficiency caused in-

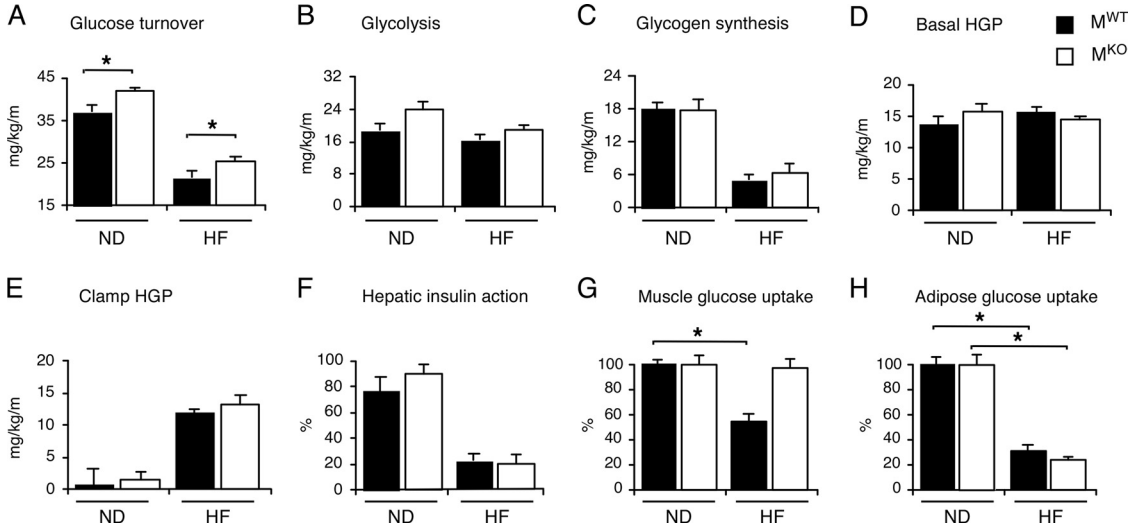

FIG. 3. Effect of muscle-specific deficiency of JNK1 on insulin sensitivity. (A to F) Insulin sensitivity was measured using a hyperinsulinemic-euglycemic clamp with conscious chow-fed (ND) and HFD-fed (HF) M^{KO} and M^{WT} mice. (A) Insulin-stimulated whole-body glucose turnover. (B) Whole-body glycolysis. (C) Whole-body glycogen plus lipid synthesis. (D) Basal HGP. (E) Insulin-stimulated rate of HGP during the clamp assay. (F) Hepatic insulin action expressed as the insulin-mediated percent suppression of basal HGP. The data presented are the means ± standard errors for approximately six to nine experiments. Statistically significant differences between M^{KO} mice and M^{WT} mice are indicated (*, $P < 0.05$). (G and H) Glucose uptake in white adipose tissue (G) and gastrocnemius muscle (H) was measured in the hyperinsulinemic-euglycemic clamp study. The data are expressed as the percent suppression of glucose uptake caused by feeding of an HFD and presented as the means ± standard errors for approximately four to nine experiments. Statistically significant differences between M^{KO} mice and M^{WT} mice are indicated (*, $P < 0.05$).

creased hepatic steatosis (Fig. 5A). Measurements of hepatic triglyceride accumulation demonstrated increased amounts of triglyceride in both chow-fed and HFD-fed M^{KO} mice compared with M^{WT} mice (Fig. 5B). The increased level of hepatic triglyceride accumulation was not accounted for by increased levels of expression of a lipogenic transcription factor/coactivator (e.g., *Srebp1*, *C/ebp*α, *C/ebp*β, and *Pgc1*β) or lipogenic genes (e.g., *Fas*) (Fig. 6). However, the triglyceride accumulation in M^{KO} mice may account for the increased levels of expression of *Tnf*α mRNA that were detected in the livers of M^{KO} mice compared to M^{WT} mice (Fig. 7).

The increased accumulation of hepatic triglyceride was associated with increased amounts of triglyceride in the blood of M^{KO} mice compared with M^{WT} mice (Fig. 8A). Triglyceride in the liver is exported to the blood in the form of serum lipoprotein (very-low-density lipoprotein [VLDL]). No significant difference in the levels of expression of microsomal triglyceride transport protein *Mttp* mRNA in the livers of M^{KO} and M^{WT} mice was detected (Fig. 6). However, increased amounts of VLDL triglyceride and decreased amounts of low-density lipoprotein and high-density lipoprotein cholesterol were found in the blood of M^{KO} mice compared with M^{WT} mice (Fig. 8B). This increased amount of VLDL triglyceride might result from decreased triglyceride hydrolysis by lipoprotein lipase (LPL). Indeed, muscle LPL is a major contributor to VLDL triglyceride hydrolysis in vivo (19), and muscle-specific *Lpl* knockout mice exhibit increased levels of VLDL triglyceride in blood and a redistribution of triglyceride to nonmuscle tissues within the body (20). Quantitative RT-PCR analysis demonstrated that *Lpl* mRNA expression in the quadriceps muscle of M^{KO} mice was reduced by 60% ± 16% compared with M^{WT} mice (mean ± standard error) ($n = 5$; $P < 0.05$), but no significant difference in *Lpl* mRNA expression levels in adipose tissues of M^{WT} and M^{WT} mice was detected ($n = 5$; $P > 0.05$). This decrease in levels of LPL expression in muscle may contribute to the increased amount of triglyceride detected in the blood and the liver of M^{KO} mice.

It is likely that the increased amount of triglyceride in the blood of M^{KO} mice may affect other tissues. To test this hypothesis, we compared adipose tissues of M^{KO} and M^{WT} mice. This analysis demonstrated that the muscle-specific JNK1 deficiency increased the HFD-induced infiltration of adipose tissue by myeloid cells (Fig. 9). Morphological analysis and immunohistochemical analysis of adipose tissue sections demonstrated increased numbers of F4/80-positive myeloid cells in HFD-fed M^{KO} mice compared with M^{WT} mice (Fig. 9A). Quantitative RT-PCR analysis of gene expression confirmed increased levels of expression of the myeloid marker genes *Lyzs* and *Cd68* (Fig. 9B). Increased levels of expression of *Icam1* and the cytokines *Il6*, *Il12*, and *Il13* (but not *Il-10*, *Tnf*α, or *Tgf*β*1*) were also detected in the adipose tissue of M^{KO} mice compared with M^{WT} mice (Fig. 9B). It was previously established that IL-13 expressed by adipocytes plays a key role in the activation of macrophages by the alternate M2a pathway (mediated by peroxisome proliferator-activated receptor γ/δ [PPARγ/δ]) that influences insulin sensitivity (5). Together, these data indicate that the muscle-specific JNK1 deficiency caused an increased inflammatory response in adipose tissue. It is possible that this response is mediated by the increased amount of triglyceride in the blood of M^{KO} mice compared with that in the blood of M^{WT} mice.

DISCUSSION

JNK1 is implicated in obesity-induced insulin resistance, metabolic syndrome, and type 2 diabetes. Thus, the treatment of mice with a JNK inhibitor decreases the concentration of

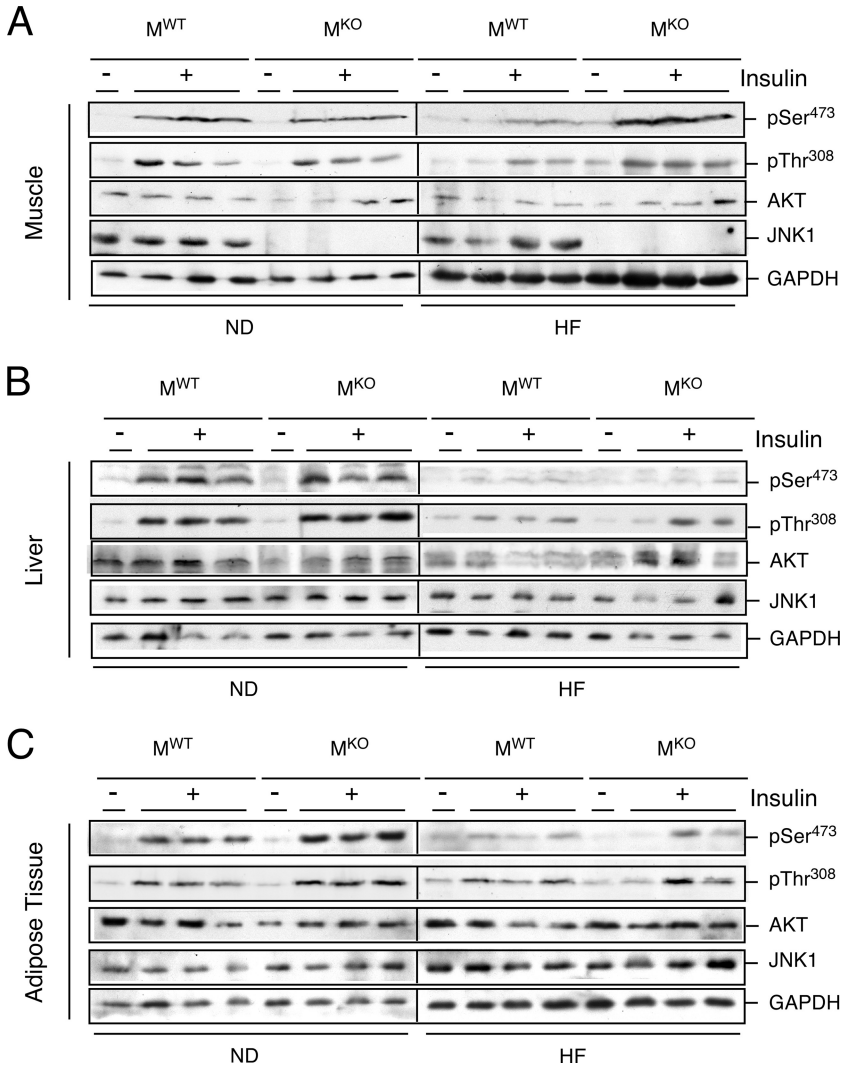

FIG. 4. Effect of muscle-specific JNK1 deficiency on insulin-stimulated AKT activation. Chow-fed (ND) and HFD-fed (HF) M^{WT} and M^{KO} mice were fasted overnight and treated by intraperitoneal injection of insulin (1.5 U/kg body mass). Extracts prepared from gastrocnemius muscle (A), liver (B), and epididymal adipose tissue (C) at 10 min postinjection were examined by immunoblot analysis with antibodies to JNK1, AKT, phospho-AKT, and GAPDH.

glucose in blood and improves insulin sensitivity (2, 9, 18). Moreover, *Jnk1*$^{-/-}$ mice are protected against HFD-induced insulin resistance (7). However, the analysis of *Jnk1*$^{-/-}$ mice is complicated because these mice fail to develop HFD-induced obesity (7). The effect of the JNK1 deficiency to protect against insulin resistance may therefore be a secondary consequence of the failure to become obese. However, recent studies using tissue-specific *Jnk1* knockout mice have provided important insights into this question. The selective ablation of the *Jnk1* gene in adipose tissue (16), liver (15), or muscle (this study) did not affect HFD-induced obesity. Nevertheless, HFD-fed mice with a selective deficiency of JNK1 in adipose tissue or muscle exhibit improved insulin sensitivity compared with control mice. These data strongly support the conclusion that JNK1 is important for the normal development of HFD-induced insulin resistance.

The regulation of insulin resistance by JNK1 is incompletely understood. It is likely that JNK1 functions are mediated by more than one mechanism. Thus, JNK1-dependent cytokine expression can contribute to inflammation-associated insulin resistance in HFD-fed mice (16). This mechanism enables JNK1 in one tissue to regulate insulin resistance in other tissues; for example, JNK1-dependent IL-6 expression by adipose tissue can mediate hepatic insulin resistance (16). JNK1 may also function by a more direct mechanism by inhibiting insulin signal transduction. One example is represented by the phosphorylation of the adapter protein IRS-1 on the negative regulatory site Ser^{307} that prevents the interaction of IRS-1 with the insulin receptor (1, 11). This mechanism may be important for the improved insulin sensitivity of adipose tissue in HFD-fed mice with an adipose-specific JNK1 deficiency (16). This conclusion is consistent with the previously reported finding that *Jnk1* gene ablation in adipose tissue suppressed IRS-1 phosphorylation on Ser^{307} (16). Similarly, the muscle-specific JNK1 deficiency decreased IRS-1 phosphorylation on Ser^{307} and improved insulin sensitivity. Indeed, the muscle-specific

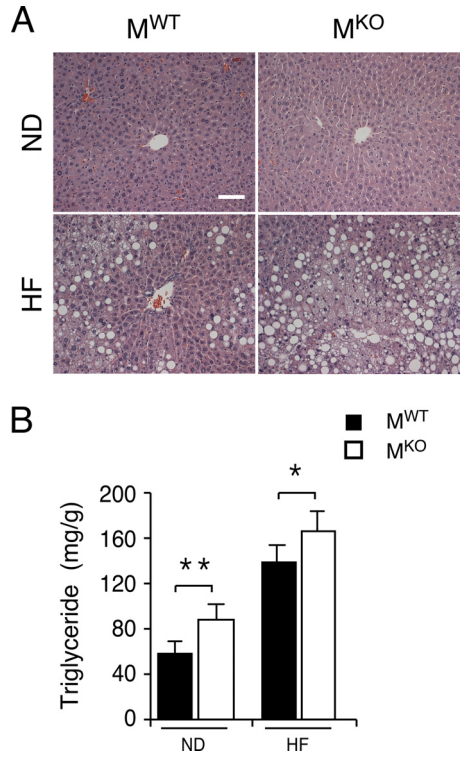

FIG. 5. Muscle-specific JNK1 deficiency causes increased diet-induced hepatic steatosis. (A) Chow-fed (ND) and HFD-fed (HF) M^{WT} and M^{KO} mice were fasted overnight. Representative sections of the liver stained with hematoxylin and eosin are presented. Scale bar, 100 μm. (B) The amount of hepatic triglyceride was measured in mice fasted overnight (means ± SD) ($n = 10$). Statistically significant differences between M^{KO} and M^{WT} are indicated (*, $P < 0.05$; **, $P < 0.01$).

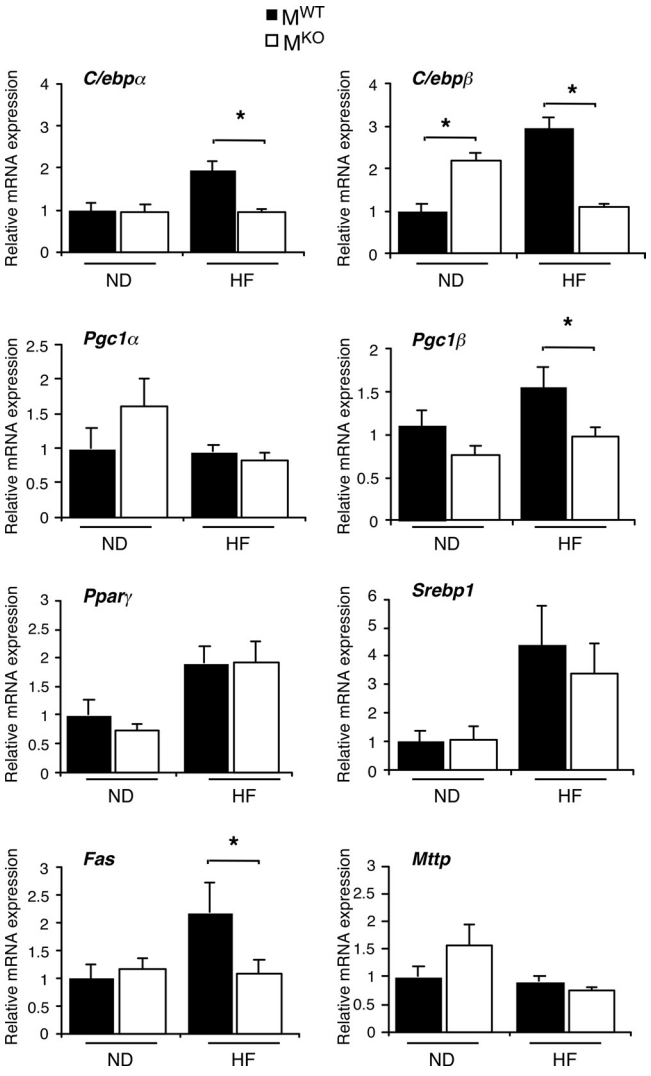

FIG. 6. Effect of muscle-specific JNK1 deficiency on hepatic lipogenic gene expression. Gene expression in the liver of chow-fed (ND) and HFD-fed (HF) M^{WT} and M^{KO} mice was measured by quantitative RT-PCR analysis of mRNA. Data for the expression of transcription factors (*C/ebpα*, *C/ebpβ*, *Pparγ*, and *Srebp1*), coactivators (*Pgc1α* and *Pgc1β*), fatty acid synthase (*Fas*), and microsomal triglyceride transfer protein (*Mttp*) mRNA are presented. The relative mRNA expression level was calculated by normalization of the data to the amount of 18S RNA in each sample (means ± SD) ($n = 6$ to ~8). Statistically significant differences are indicated (*, $P < 0.05$).

JNK1 deficiency protected insulin-stimulated AKT activation selectively in muscle, but not liver or adipose tissue, after feeding of an HFD. This observation suggests that JNK1 in muscle can regulate insulin resistance by a cell-autonomous mechanism that involves, at least in part, the negative regulatory phosphorylation of IRS-1. This conclusion is consistent with the results of a recently reported study that demonstrated an improved insulin sensitivity of transgenic mice that expressed a phosphorylation-defective IRS-1 protein in muscle (13).

One unexpected consequence of the muscle-specific JNK1 deficiency was the finding that the triglyceride concentration in blood of M^{KO} mice was greater than that in blood of M^{WT} mice. The mechanism that accounts for the increase in the concentration of triglyceride in blood is unclear. However, a reduced level of expression of muscle LPL may represent one contributing factor. It was previously established that muscle LPL acts to hydrolyze VLDL triglyceride (19). A recent report demonstrated that a muscle-specific LPL deficiency caused an increase in blood triglyceride concentrations and the redistribution of triglyceride to nonmuscle tissues within the body (20). A consequence of the redistribution of triglyceride in these LPL-deficient mice is an increased insulin sensitivity in muscle but a decreased insulin sensitivity in other tissues, including liver and adipose tissue (20). These data suggest that the redistribution of triglyceride may contribute to the phenotype of muscle-specific JNK1-deficient mice and that reduced muscle LPL expression levels may represent one factor that mediates the increased muscle insulin sensitivity of HFD-fed M^{KO} mice. However, unlike chow-fed muscle-specific-LPL-deficient mice, chow-fed M^{KO} mice did not exhibit decreased insulin sensitivity in muscle and adipose tissue; this is most likely because the reduction in muscle LPL expression levels in M^{KO} mice differs from the complete absence of muscle LPL in LPL-deficient mice. Nonetheless, the reduced level of LPL expression in muscle of M^{KO} mice may contribute to the increased triglyceride accumulation in blood and liver and in-

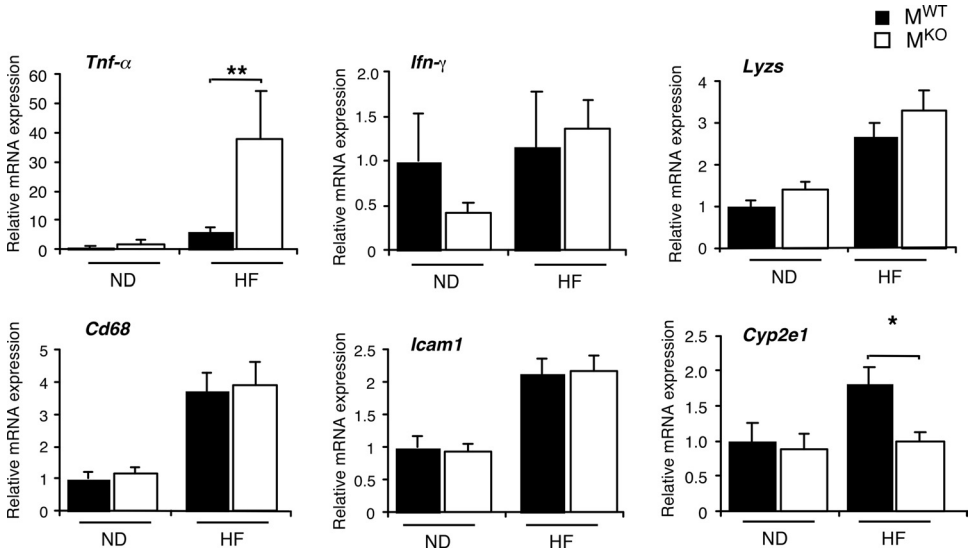

FIG. 7. Effect of muscle-specific JNK1 deficiency on hepatic inflammatory gene expression. Gene expression in the liver of chow-fed (ND) and HFD-fed (HF) M^{WT} and M^{KO} mice fasted overnight was measured by quantitative RT-PCR analysis of mRNA (TaqMan assays). Data for the expression of *Tnfα*, *Il6*, *Ifnγ*, *Cd68*, *Icam1*, *Lyzs*, and cytochrome p450 2E1 (*Cye2e1*) mRNAs are presented. The relative mRNA expression level was calculated by normalization of the data to the amount of 18S RNA in each sample (means ± SD) (n = 6 to ~8). Statistically significant differences are indicated (*, $P < 0.05$; **, $P < 0.01$).

creased inflammation of adipose tissue, particularly in HFD-fed mice.

Together, the results of this study provide insight into the mechanism of JNK1-mediated insulin resistance. These data indicate that the protection of *Jnk1*$^{-/-}$ mice against the effects of feeding an HFD represents a complex phenotype that is derived from effects of JNK1 in multiple tissues. The protection against HFD-induced obesity observed in studies of

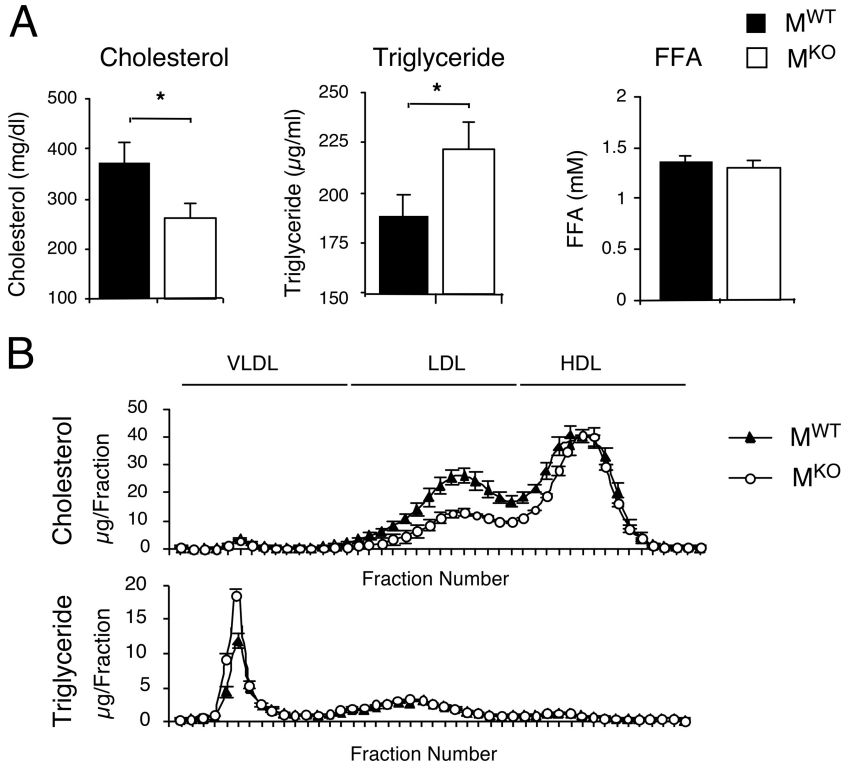

FIG. 8. Effect of muscle-specific JNK1 deficiency on blood lipids. (A) HFD-fed M^{WT} and M^{KO} mice were fasted overnight. The amounts of cholesterol, triglyceride, and free fatty acid (FFA) in the blood were measured (means ± SD) (n = 10). Statistically significant differences between M^{KO} and M^{WT} are indicated (*, $P < 0.05$). (B) Analysis of VLDL, low-density lipoprotein (LDL), and high-density lipoprotein (HDL) in the sera of HFD-fed M^{WT} and M^{KO} mice. Fast-performance liquid chromatography profiles of cholesterol (top) and triglyceride (bottom) are presented (means ± SD) (n = 10).

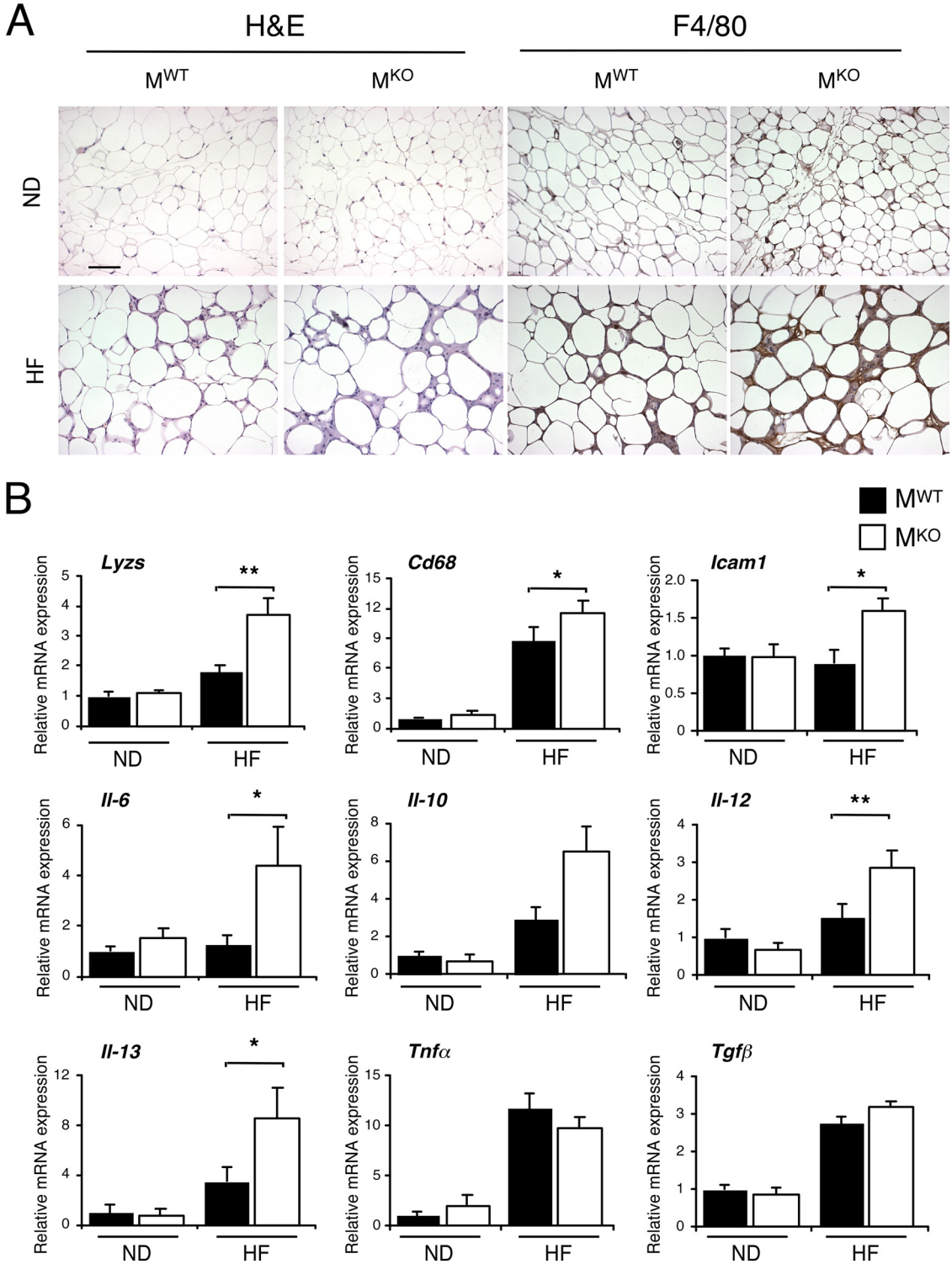

FIG. 9. Muscle-specific JNK1 deficiency causes increased diet-induced inflammation of adipose tissue. (A) Chow-fed (ND) and HFD-fed (HF) M^{WT} and M^{KO} mice were fasted overnight. Representative histological sections of epididymal adipose tissue stained with hematoxylin and eosin (left panels) and with an antibody (F4/80) to a macrophage marker (right panels) are presented. Scale bar, 100 μm. (B) Gene expression in epididymal adipose tissue was measured by quantitative RT-PCR analysis of mRNA. The relative mRNA expression level was calculated by normalization of the data to the amount of *Gapdh* mRNA in each sample (means ± SD) ($n = 6$ to ~8). Statistically significant differences are indicated (*, $P < 0.05$; **, $P < 0.01$).

Jnk1$^{-/-}$ mice is not accounted for by a JNK1 deficiency in adipose tissue (16), liver (15), or muscle (this study). JNK1 in adipose tissue is required for HFD-induced insulin resistance in adipose tissue and liver (16). However, JNK1 in liver is not required for HFD-induced hepatic insulin resistance (15). Here we demonstrate that JNK1 in muscle is required for HFD-induced muscle insulin resistance. This analysis indicates that the overall phenotype of *Jnk1*$^{-/-}$ mice represents a complicated mixture of separate phenotypes caused by a JNK1 deficiency in different tissues.

ACKNOWLEDGMENTS

We thank D. Lee and P. Tso for the analysis of blood lipoproteins (Mouse Metabolic Phenotyping Center, University of Cincinnati); M. Das for providing the floxed *Jnk1* mice; V. Benoit, J. Reilly, and J.-H. Liu for expert technical assistance; and K. Gemme for administrative assistance.

These studies were supported by grants from the National Institutes of Health (grants CA65861 to R.J.D. and DK80756 to J.K.K.) and the American Diabetes Association (grant 7-07-RA-80 to J.K.K.). The UMass Mouse Phenotyping Center is supported by the NIDDK Diabetes and Endocrinology Research Center (grant DK52530). R.J.D. is an Investigator of the Howard Hughes Medical Institute.

REFERENCES

1. **Aguirre, V., T. Uchida, L. Yenush, R. Davis, and M. F. White.** 2000. The c-Jun NH(2)-terminal kinase promotes insulin resistance during association with insulin receptor substrate-1 and phosphorylation of Ser(307). J. Biol. Chem. **275:**9047–9054.
2. **Bennett, B. L., Y. Satoh, and A. J. Lewis.** 2003. JNK: a new therapeutic target for diabetes. Curr. Opin. Pharmacol. **3:**420–425.
3. **Bruning, J. C., M. D. Michael, J. N. Winnay, T. Hayashi, D. Horsch, D. Accili, L. J. Goodyear, and C. R. Kahn.** 1998. A muscle-specific insulin receptor knockout exhibits features of the metabolic syndrome of NIDDM without altering glucose tolerance. Mol. Cell **2:**559–569.
4. **Das, M., F. Jiang, H. K. Sluss, C. Zhang, K. M. Shokat, R. A. Flavell, and R. J. Davis.** 2007. Suppression of p53-dependent senescence by the JNK signal transduction pathway. Proc. Natl. Acad. Sci. U. S. A. **104:**15759–15764.
5. **Desvergne, B.** 2008. PPARdelta/beta: the lobbyist switching macrophage allegiance in favor of metabolism. Cell Metab. **7:**467–469.
6. **Dong, C., D. D. Yang, M. Wysk, A. J. Whitmarsh, R. J. Davis, and R. A. Flavell.** 1998. Defective T cell differentiation in the absence of Jnk1. Science **282:**2092–2095.
7. **Hirosumi, J., G. Tuncman, L. Chang, C. Z. Gorgun, K. T. Uysal, K. Maeda, M. Karin, and G. S. Hotamisligil.** 2002. A central role for JNK in obesity and insulin resistance. Nature **420:**333–336.
8. **Kahn, S. E., R. L. Hull, and K. M. Utzschneider.** 2006. Mechanisms linking obesity to insulin resistance and type 2 diabetes. Nature **444:**840–846.
9. **Kaneto, H., Y. Nakatani, T. Miyatsuka, D. Kawamori, T. A. Matsuoka, M. Matsuhisa, Y. Kajimoto, H. Ichijo, Y. Yamasaki, and M. Hori.** 2004. Possible novel therapy for diabetes with cell-permeable JNK-inhibitory peptide. Nat. Med. **10:**1128–1132.
10. **Kim, H. J., T. Higashimori, S. Y. Park, H. Choi, J. Dong, Y. J. Kim, H. L. Noh, Y. R. Cho, G. Cline, Y. B. Kim, and J. K. Kim.** 2004. Differential effects of interleukin-6 and -10 on skeletal muscle and liver insulin action in vivo. Diabetes **53:**1060–1067.
11. **Lee, Y. H., J. Giraud, R. J. Davis, and M. F. White.** 2003. c-Jun N-terminal kinase (JNK) mediates feedback inhibition of the insulin signaling cascade. J. Biol. Chem. **278:**2896–2902.
12. **Mora, A., K. Sakamoto, E. J. McManus, and D. R. Alessi.** 2005. Role of the PDK1-PKB-GSK3 pathway in regulating glycogen synthase and glucose uptake in the heart. FEBS Lett. **579:**3632–3638.
13. **Morino, K., S. Neschen, S. Bilz, S. Sono, D. Tsirigotis, R. M. Reznick, I. Moore, Y. Nagai, V. Samuel, D. Sebastian, M. White, W. Philbrick, and G. I. Shulman.** 2008. Muscle-specific IRS-1 Ser→Ala transgenic mice are protected from fat-induced insulin resistance in skeletal muscle. Diabetes **57:**2644–2651.
14. **Perseghin, G., K. Petersen, and G. I. Shulman.** 2003. Cellular mechanism of insulin resistance: potential links with inflammation. Int. J. Obes. Relat. Metab. Disord. **27**(Suppl. 3)**:**S6–S11.
15. **Sabio, G., J. Cavanagh-Kyros, H. J. Ko, D. Y. Jung, S. Gray, J. Y. Jun, T. Barrett, A. Mora, J. K. Kim, and R. J. Davis.** 2009. Prevention of steatosis by hepatic JNK1. Cell Metab. doi:10.1016/j.cmet.2009.09.007.
16. **Sabio, G., M. Das, A. Mora, Z. Zhang, J. Y. Jun, H. J. Ko, T. Barrett, J. K. Kim, and R. J. Davis.** 2008. A stress signaling pathway in adipose tissue regulates hepatic insulin resistance. Science **322:**1539–1543.
17. **Savage, D. B., K. F. Petersen, and G. I. Shulman.** 2007. Disordered lipid metabolism and the pathogenesis of insulin resistance. Physiol. Rev. **87:**507–520.
18. **Stebbins, J. L., S. K. De, T. Machleidt, B. Becattini, J. Vazquez, C. Kuntzen, L. H. Chen, J. F. Cellitti, M. Riel-Mehan, A. Emdadi, G. Solinas, M. Karin, and M. Pellecchia.** 2008. Identification of a new JNK inhibitor targeting the JNK-JIP interaction site. Proc. Natl. Acad. Sci. U. S. A. **105:**16809–16813.
19. **Wang, H., and R. H. Eckel.** 2009. Lipoprotein lipase: from gene to obesity. Am. J. Physiol. Endocrinol. Metab. **297:**E271–E288.
20. **Wang, H., L. A. Knaub, D. R. Jensen, D. Y. Jung, E. G. Hong, H. J. Ko, A. M. Coates, I. J. Goldberg, B. A. de la Houssaye, R. C. Janssen, C. E. McCurdy, S. M. Rahman, C. S. Choi, G. I. Shulman, J. K. Kim, J. E. Friedman, and R. H. Eckel.** 2009. Skeletal muscle-specific deletion of lipoprotein lipase enhances insulin signaling in skeletal muscle but causes insulin resistance in liver and other tissues. Diabetes **58:**116–124.
21. **Weston, C. R., and R. J. Davis.** 2007. The JNK signal transduction pathway. Curr. Opin. Cell Biol. **19:**142–149.
22. **Whitmarsh, A. J., and R. J. Davis.** 2001. Analyzing JNK and p38 mitogen-activated protein kinase activity. Methods Enzymol. **332:**319–336.
23. **Yang, R., and J. M. Trevillyan.** 2008. c-Jun N-terminal kinase pathways in diabetes. Int. J. Biochem. Cell Biol. **40:**2702–2706.